Endosomal clathrin drives actin accumulation at the immunological synapse

Carmen Calabia-Linares[1], Javier Robles-Valero[1], Hortensia de la Fuente[1], Manuel Perez-Martinez[1], Noa Martín-Cofreces[1,2], Manuel Alfonso-Pérez[1], Cristina Gutierrez-Vázquez[2], María Mittelbrunn[2], Sales Ibiza[2], Francisco R. Urbano-Olmos[3], Covadonga Aguado-Ballano[3], Carlos Oscar Sánchez-Sorzano[4], Francisco Sanchez-Madrid[1,5] and Esteban Veiga[1,5,6,*]

[1]Servicio de Inmunología, Hospital Universitario de la Princesa, Instituto de Investigación Sanitaria Hospital de la Princesa (IP), Diego de León, 62, 28006 Madrid, Spain
[2]Department Biología Vascular e Inflamación, Centro Nacional de Investigaciones Cardiovasculares, Melchor Fernández Almagro s/n, 28029 Madrid, Spain
[3]Laboratorio de Microscopía Electrónica de Transmisión, Facultad de Medicina, Universidad Autónoma de Madrid, Arzobispo Morcillo s/n, 28029 Madrid, Spain
[4]Unidad de Biocomputación, Centro Nacional de Biotecnología (CSIC), Campus Universidad Autónoma s/n, 28049 Cantoblanco, Madrid
[5]Facultad de Medicina, Universidad Autónoma de Madrid, 28029 Madrid, Spain
[6]Centro Nacional de Biotecnología (CSIC), Campus Universidad Autónoma s/n, 28049 Cantoblanco, Madrid
*Author for correspondence (eveiga@cnb.csic.es)

Accepted 4 November 2010
Journal of Cell Science 124, 820-830

doi:10.1242/jcs.078832

Summary

Antigen-specific cognate interaction of T lymphocytes with antigen-presenting cells (APCs) drives major morphological and functional changes in T cells, including actin rearrangements at the immune synapse (IS) formed at the cell–cell contact area. Here we show, using cell lines as well as primary cells, that clathrin, a protein involved in endocytic processes, drives actin accumulation at the IS. Clathrin is recruited towards the IS with parallel kinetics to that of actin. Knockdown of clathrin prevents accumulation of actin and proteins involved in actin polymerization, such as dynamin-2, the Arp2/3 complex and CD2AP at the IS. The clathrin pool involved in actin accumulation at the IS is linked to multivesicular bodies that polarize to the cell–cell contact zone, but not to plasma membrane or Golgi complex. These data underscore the role of clathrin as a platform for the recruitment of proteins that promote actin polymerization at the interface of T cells and APCs.

Key words: Actin, Clathrin, Cytoskeleton, Immunological synapse

Introduction

T cells have a central role in adaptive immunity, either by enhancing or suppressing immune responses through antigen-triggered cytokine secretion or by destroying antigen-bearing cells (Friedl et al., 2005). T cells are activated by the establishment of cell–cell contacts with antigen-presenting cells (APCs) such as dendritic cells (DCs), macrophages or B cells (Friedl et al., 2005; Reichardt et al., 2007). These contacts, which involve recognition of antigen-bearing MHC molecules on APCs by the T-cell receptor (TCR), are known as immunological synapses (ISs) (Billadeau et al., 2007; Friedl et al., 2005; Vicente-Manzanares and Sanchez-Madrid, 2004). The IS is highly dynamic and in its more structured form is organized into concentric rings of multimolecular assemblies. The central region, called the central supramolecular activation cluster (cSMAC), contains the clustered MHC-conjugated TCR complexes, including CD3, together with the co-stimulator CD28 and other signaling molecules; surrounding this structure is a ring of adhesion molecules called the peripheral supramolecular activation cluster (pSMAC), which includes the integrins LFA-1 (integrin $\alpha L\beta 2$) and VLA-4 (integrin $\alpha 4\beta 1$) (Dustin, 2009; Mittelbrunn et al., 2004). TCR stimulation during immune synapsing triggers major morphological and functional changes in T cells, including a large-scale accumulation of actin, which increases the area of T cell and APC interaction (Billadeau et al., 2007; Vicente-Manzanares and Sanchez-Madrid, 2004). Actin polymerization defects result in impaired T cell activation and deregulation of cytokine secretion (Nolz et al., 2007), demonstrating that these actin rearrangements are absolutely necessary for productive IS formation and lymphocyte activation.

Signaling initiated at the IS involves numerous TCR-proximal kinases and adaptor molecules whose actions culminate in the activation of the Arp2/3 complex, which promotes actin nucleation and polymerization, as well as branching of actin filaments (Billadeau et al., 2007; Vicente-Manzanares and Sanchez-Madrid, 2004). Arp2/3 activators identified at the IS include the Wiskott–Aldrich syndrome protein (WASP), Hs1 (cortactin homolog) and WAVE2 (Billadeau et al., 2007). Moreover, the large GTPase dynamin-2 has recently been shown to be recruited to the IS, where it regulates the reorganization of F-actin (Gomez et al., 2005). Nevertheless, the initial link between TCR activation and actin polymerization at the IS remains elusive.

In many aspects, the signaling and cytoskeletal rearrangements triggered by TCR activation at the IS resemble events that occur in other systems, such as lamellipodium formation at the advancing zone of migrating cells, or the contact zones formed between pathogens and host cells. For example, the receptor-activated signaling pathways that lead to actin polymerization during bacterial infection, similarly to those occurring at the IS, involve Arp2/3, N-WASP, WAVE, CD2AP (CD2-associated protein) and dynamin-2, among other proteins (Hamon et al., 2006; Veiga and Cossart,

Journal of Cell Science

2005). Interestingly, it has been recently demonstrated that clathrin, which is well known for its central role in endocytic processes, has a determining role in actin remodelling during bacterial and fungal infections (Veiga and Cossart, 2005; Veiga et al., 2007). These studies suggest that membranes coated with clathrin might serve as a molecular platform for recruitment of the protein machinery necessary to trigger localized actin polymerization during pathogen invasion. This hypothesis, together with the work of others (Yarar et al., 2005) challenged the classical view of clathrin-mediated endocytosis, which in mammalian cells was assumed to occur independently of actin (Conner and Schmid, 2003). Clathrin functions by binding to cell membranes through interaction with proteins called clathrin adaptors (Owen et al., 2004). The association of clathrin with the plasma membrane during endocytosis has been extensively studied (Conner and Schmid, 2003; Ungewickell and Hinrichsen, 2007). Clathrin is also detected in intracellular compartments, associated mainly with the Golgi complex (Jaiswal et al., 2009), where it is also involved in vesicle formation, and with late endosomes known as multivesicular bodies (MVBs) (Murk et al., 2003; Raiborg et al., 2002; Raiborg et al., 2006). MVBs form characteristic structures of vesicles within vesicles that can be detected by electron microscopy (Murk et al., 2003; Raiborg et al., 2002). Endocytic vesicles containing activated receptors are recognized by ESCRT complexes, four protein complexes (0, I, II, III, IV) that work in tandem to promote the internalization of the cargo-containing vesicles into the MVB (Slagsvold et al., 2006). These MVBs are able to fuse with lysosomes, thereby degrading the endocytic cargo (Hanson et al., 2009; Williams and Urbe, 2007). Recently, it has been described that TSG101, which forms part of ESCRT-I, regulates IS structure (Vardhana et al., 2010). Moreover, lyso-bis-phosphatidic acid, which is typically found in MVBs (Kobayashi et al., 1998), was detected at the cSMAC (Varma et al., 2006), suggesting that some interactions might occur between MVBs and the IS. However, whether MVBs polarize to the IS needs corroboration, and the functional roles that MVBs have at the IS remain unknown. Here, we demonstrate that clathrin accumulates and regulates actin rearrangements at the IS in T cells. We additionally show that clathrin is required for the recruitment of proteins involved in actin polymerization such as dynamin-2, the Arp2/3 complex and CD2AP. We also show that the clathrin pool involved in actin accumulation at the IS is associated with MVBs, which polarize to the IS, and not to plasma membrane or Golgi complex.

Results

Clathrin polarizes towards the immunological synapse

We first examined clathrin localization in conjugates of T cells and APCs. Jurkat T cells bearing the TCR Vβ8 chain recognize the staphylococcal enterotoxin E (SEE) superantigen bound to MHC class II in Raji APCs (Montoya et al., 2002). Upon stimulation of Jurkat T cells with SEE-loaded APCs, endogenous T cell clathrin relocalized and accumulated at the IS, as revealed by immunofluorescence using antibodies against the clathrin heavy chain (Fig. 1A). TCR stimulation by SEE-loaded APCs was confirmed by the clustering of CD3 at the cSMAC (Fig. 1A).

To quantify clathrin accumulation in individual immune synapses, we developed new algorithms and software, called ‘Synapse Measures’, which can be used as a plug-in for ImageJ (http://rsbweb.nih.gov/ij/) and which will be made freely available. By analyzing and comparing fluorescence signals from several small regions in the T cell, the APC and in the IS, this program estimates the contribution of background fluorescence and the constitutive fluorescence of cell borders, thereby yielding more accurate measurements of localized immunofluorescence. A detailed description of the Synapse Measures program, including the algorithms used, is included in the Materials and Methods. Using this method, we were able to accurately quantify the ratio between the immunofluorescence intensity of T cell clathrin (and other proteins) at the IS with that remained in the rest of the T cell (Fig. 1B). The concentration of clathrin at the IS increased 2.6-fold when the TCR was stimulated with antigen (Fig. 1C; each dot in the figure corresponds to a single IS). A fluorescently tagged clathrin light chain fused to td-Tomato (td-Tomato–Lca) (Massol et al., 2006) also accumulated at the IS (Fig. 1D), validating its use for dynamics studies. The time courses of the recruitment of clathrin (td-Tomato–LCa) and actin (GFP–actin) (Boyer et al., 2006) to the IS were monitored by fast acquisition (~0.9 second intervals) of confocal stacks from live cells, using a Leica TCS-SP5 microscope equipped with a resonant scanner (Fig. 1E and supplementary material Movie 1). Over the period examined, the kinetics of clathrin accumulation at the IS mirrored that of actin (Fig. 1F).

To ascertain whether clathrin polarizes to the IS in a more physiological setting, we used conjugates formed by primary T cells obtained from peripheral blood lymphocytes (PBLs) of healthy human donors. To enrich the heterogeneous population of PBLs in T cells harbouring the TCR Vβ8 chain (which is able to recognize the SEE), the PBLs were treated with SEE, IL-2 and phytohaematogglutinin (PHA). This treatment selectively expanded the T cell population responding to SEE. We used Raji cells as APCs and primary DCs derived from monocytes obtained from healthy human donors. We examined clathrin localization in T-cell–APC conjugates. Clathrin from primary T cells bearing TCR Vβ8 chain relocalized and accumulated at the IS upon T cell stimulation with either Raji or primary DCs loaded with SEE, as revealed by immunofluorescence using antibodies against the clathrin heavy chain (Fig. 2A,B). TCR stimulation by SEE-loaded APCs was confirmed by the clustering of TCR at the IS (Fig. 2A,B). Quantification of clathrin accumulation using the Synapse Measures plug-in confirmed that the concentration of clathrin at the IS increased more than twofold when the TCR from primary T cells was antigen stimulated by both Raji and primary DCs (Fig. 2C).

Clathrin is necessary for actin accumulation at the immunological synapse

The role of clathrin in actin accumulation at the IS was examined by siRNA knockdown (KD) of clathrin heavy chain in Jurkat T cells. Reduced expression of clathrin was confirmed by fluorescence (Fig. 3A) and immunoblot (Fig. 3B). Note that clathrin reduction did not affect cell viability nor cell division rate (data not shown). In the presence of SEE-loaded APCs, clathrin-depleted T cells, which present the same levels of total actin that cells with normal amounts of clathrin (Fig. 3B), were unable to polymerize actin at the IS (Fig. 3A). However, CD3 accumulation at the T-cell–APC contact site appeared to be unaffected, suggesting that T cell activation is not impaired by partial depletion of clathrin (Fig. 3A, right). The frequency of T-cell–Raji conjugate formation measured by immunofluorescence (not shown), or by flow cytometry (looking for double positives: $CD3^+$ for T cells and cellular marker CMTMR for Raji cells) was variable and dependent of the experiment, but showed no significant differences between control and clathrin-

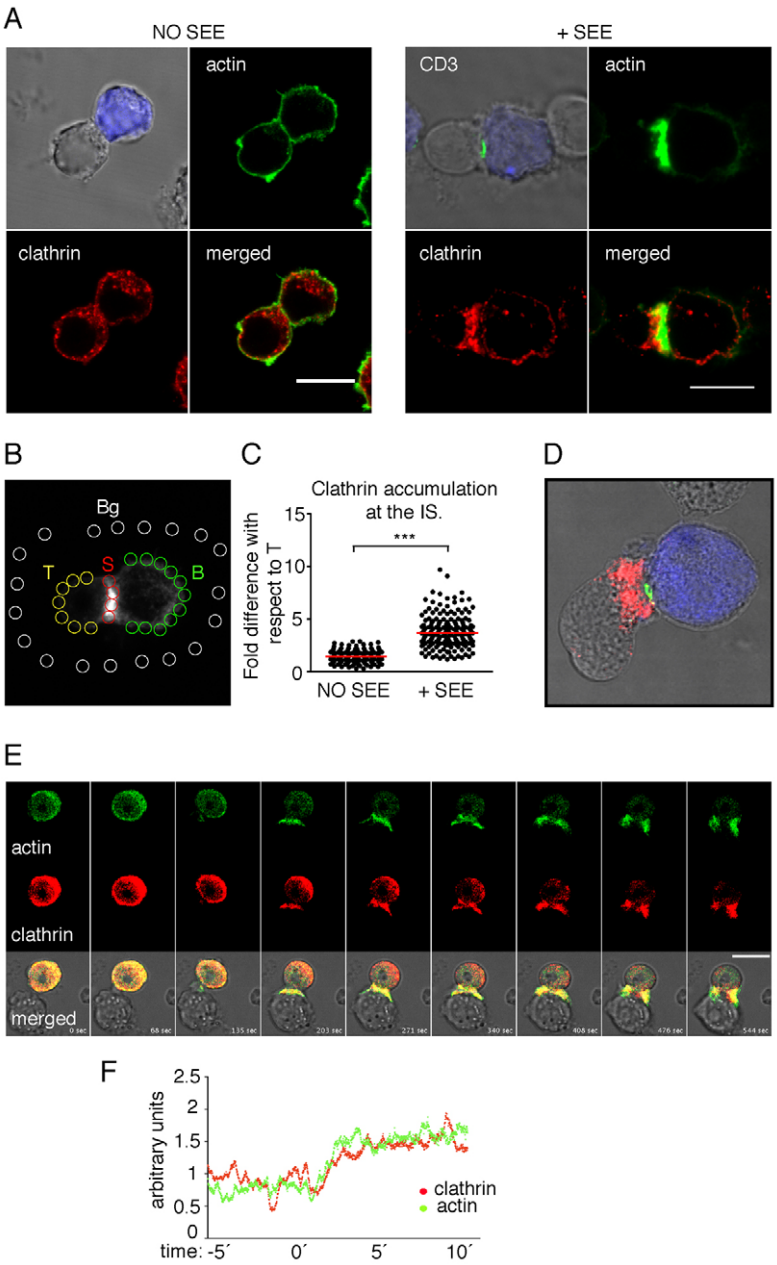

Fig. 1. Clathrin accumulates at the IS. (**A**) T cells conjugated with unloaded Raji APCs (left) or antigen (SEE)-loaded APCs (right). The combined fluorescent and phase contrast images show the T cell (not stained), the CMAC-stained APC (blue) and CD3 immunofluorescence (green); note that CD3 accumulates at the cell–cell contact site only when the APC is loaded with antigen. In the confocal immunofluorescence images, actin is shown in green and clathrin in red. Merged images show fluorescence corresponding to actin and clathrin. Clathrin antibody used was rabbit polyclonal raised against clathrin heavy chain. (**B**) Maximal projection image from confocal stacks of a clathrin immunostained T cell–APC conjugate analyzed with the Synapse Measures program. *Bg*, background signal; *B*, signal from the APC; *T*, signal from the T cell (not at the synapse); *S*, signal from the synapse. Clathrin from both T cell and APC contribute to S. The algorithms used are explained in the Materials and Methods. (**C**) Clathrin accumulation at the IS measured using Synapse Measures. Each dot represents the relative intensity of clathrin immunofluorescence in an individual T-cell–APC contact, analyzed as in B. More than 300 intercellular contacts were analyzed in three independent experiments. ***P<0.005 (Mann–Whitney test). Red lines indicate the median values. (**D**) Combination fluorescence and phase-contrast image showing an APC-conjugated T cell expressing td-Tomato-tagged clathrin light chain. td-Tomato–LCa (clathrin) is shown in red, endogenous CD3 in green, and the antigen-primed APC in blue; the T cell is not stained. (**E**) Confocal time series showing a T cell transiently expressing td-Tomato–LCa (red) and GFP–actin (green) contacting an antigen-primed APC (not colored). The figure shows one of every 70 acquisition frames from supplementary material Movie 1, giving an approximate interval between images of 68 seconds. (**F**) Fluorescence intensity profiles from supplementary material Movie 1 for td-Tomato–LCa and GFP–actin fluorescence in a region of interest in the T cell near the APC. Values were normalized to the maximum signal. Scale bars: 10 µm.

knockdown (KD) Jurkat T cells (supplementary material Fig. S1A). Actin dynamics in clathrin KD T cells expressing GFP–actin was monitored by live-cell imaging using a Leica multidimensional microscope. Clathrin KD T cells were unable to accumulate GFP–actin to the IS (supplementary material Movie 2).

Quantification of actin accumulation with Synapse Measures confirmed that clathrin-depleted T cells were unable to accumulate actin at the IS (Fig. 3C). These data were confirmed using a different set of four clathrin heavy chain siRNAs (not shown). Clathrin relocalization in T-cell–APC conjugates was unaffected by the presence of cytochalasin D, which disrupts actin filaments, indicating that clathrin accumulation at the IS in T cells is independent of actin (Fig. 3D).

As the observed decrease in actin polymerization at the IS could be due to reduced levels of relevant receptors for TCR signaling and IS formation, as a control we further tested the effect of clathrin KD on T cell activation and surface expression of receptors implicated in IS signaling by flow cytometry. Surface levels of TCR, CD3, CD28, CD4, LFA-1 and VLA-4 were not reduced by clathrin depletion (Fig. 4A). CD3 surface expression was slightly increased within clathrin KD T cells, indicating that at least part of the CD3 population is constitutively removed from the plasma membrane by clathrin-mediated endocytosis. In addition, clathrin KD did not affect the increased surface expression of CD69, an early marker of T cell activation, observed upon stimulation of T cells with anti-CD3 and anti-CD28 antibodies (Fig. 4B). Likewise, clathrin depletion did not inhibit the rapid phosphorylation of PLCγ, Zap70 and ERK induced by antibody stimulation (Fig. 4C). Moreover, the levels of protein phosphorylation after antibody stimulation were slightly higher in clathrin KD T cells (Fig. 4D). Note that experiments shown in Fig. 3 were done in parallel (with the same samples) with those shown in Fig. 4.

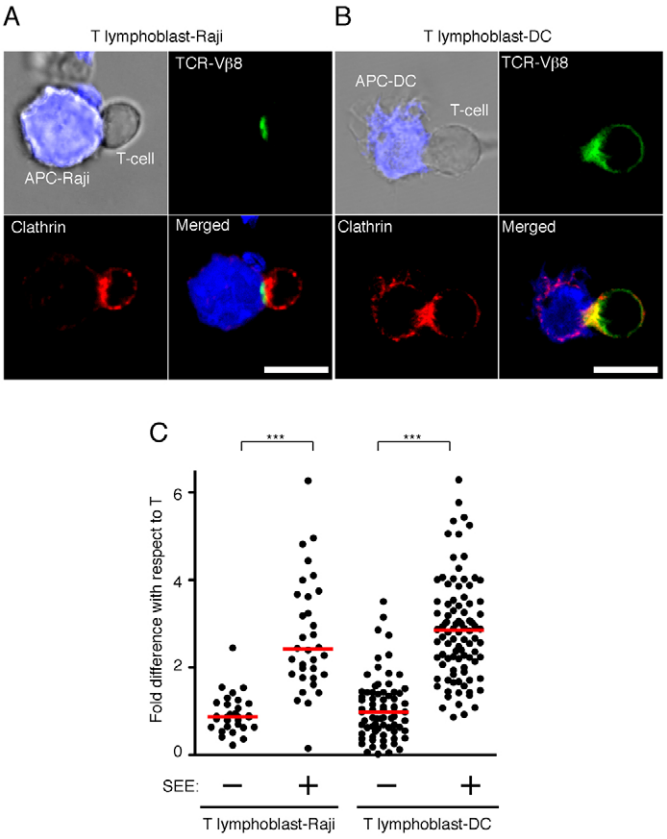

Fig. 2. Clathrin accumulates at the IS in primary lymphoblasts. (**A**,**B**) T lymphoblasts conjugated with SEE-loaded APCs (Raji, A; DCs, B). The combined fluorescent and phase-contrast images show the T lymphoblasts (not colored), and CMAC-stained APC (blue). TCR harbouring the Vβ8 chain is shown in green and clathrin in red. Merged images show fluorescence corresponding to clathrin, TCR and APCs. Clathrin antibody used was rabbit polyclonal raised against clathrin heavy chain and TCR was detected with an anti-Vβ8 chain. Scale bars: 10 µm. (**C**) Clathrin accumulation at the IS measured using Synapse Measures program. Each dot represents the relative intensity of clathrin immunofluorescence in an individual T-cell–APC contact. For each type of conjugate (Raji or DC) more than 50 intercellular contacts were analyzed in three independent experiments. T lymphoblasts were collected from four healthy donors; DCs were collected from three healthy donors. ***P<0.005 (Mann–Whitney test). Red lines indicate the median values.

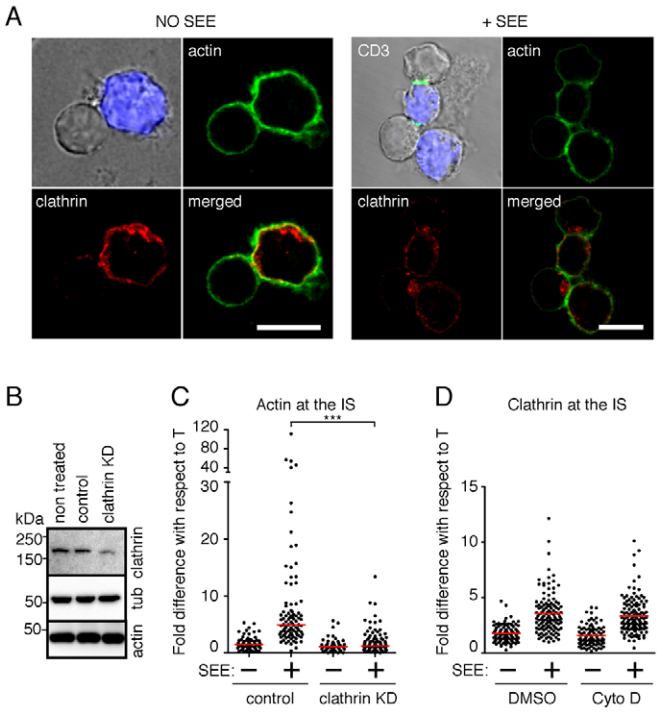

Fig. 3. Clathrin is necessary for actin accumulation at the IS. (**A**) Clathrin-depleted Jurkat T cells conjugated with unloaded Raji APCs (left) or antigen (SEE)-loaded APCs (right). The combined fluorescent and phase contrast images show the T cell (not stained), the APC (blue) and CD3 immunofluorescence (green); note that CD3 accumulation at the contact with the antigen-primed APC is unaffected by clathrin depletion. In the confocal immunofluorescence images, actin is shown in green and clathrin in red. Clathrin antibody used was rabbit polyclonal raised against clathrin heavy chain. Merged images show fluorescence corresponding to actin and clathrin. Scale bars: 10 µm (**B**) Immunoblot showing suppression of clathrin protein expression in clathrin-knockdown (KD) T cells. Total actin and tubulin (tub) are shown as loading controls. (**C**) Quantitative analysis of actin accumulation at the cell–cell contact with Synapse Measures program. Control or clathrin KD T cells were conjugated with superantigen (SEE)-loaded (+) or unloaded (–) APCs. Each dot represents the relative actin immunofluorescence intensity in an individual T-cell–APC contact. More than 300 intercellular contacts were analyzed in three independent experiments. ***P<0.005 (Mann–Whitney test). Red lines indicate the median values. (**D**) T cells treated with DMSO (control) or cytochalasin D were conjugated with SEE-loaded (+) or unloaded (–) APCs, and clathrin accumulation in the at the cell–cell contact site was analyzed with Synapse Measures program. Each dot represents the relative clathrin immunofluorescence intensity in an individual T-cell–APC contact. More than 400 intercellular contacts were analyzed in three independent experiments. No significant differences (Mann–Whitney test) were found between control and cytochalasin-D-treated T cells.

To assess the functional consequences of the effect of clathrin silencing on the physiology of the T cells, we measured the secretion of IL-2. It has been shown that reducing actin polymerization at the IS, either by using drugs, or by depleting actin-binding proteins, alters the secretion of IL-2 (Nolz et al., 2007; Perez-Martinez et al., 2010). Clathrin reduction deregulates IL-2 secretion (supplementary material Fig. S1B), in a similar way to that observed by others using low doses of cytochalasin D (Nolz et al., 2007).

Clathrin is necessary for recruitment of key adaptor and regulatory proteins involved in actin polymerization to the immunological synapse

To investigate the possibility that clathrin serves as a molecular platform for the recruitment of actin-polymerizing proteins, we assessed the role of clathrin in the recruitment of the large GTPase dynamin-2, which promotes actin polymerization at the IS (Gomez et al., 2005). Time-lapse confocal analysis of T-cell–APC conjugates showed that dynamin-2 and clathrin relocate to the IS at the same rate (Fig. 5A and supplementary material Movie 3); moreover, clathrin and dynamin-2 accumulated at the same areas of the IS (Fig. 5A,B). By contrast, clathrin-depleted T cells were unable to accumulate dynamin-2 when challenged with SEE-loaded APCs (Fig. 5B, bottom panels and Fig. 5C). Clathrin depletion also impaired the recruitment towards the IS of Arp2/3 complex (Fig. 5D). CD2AP, another important mediator of TCR-induced actin

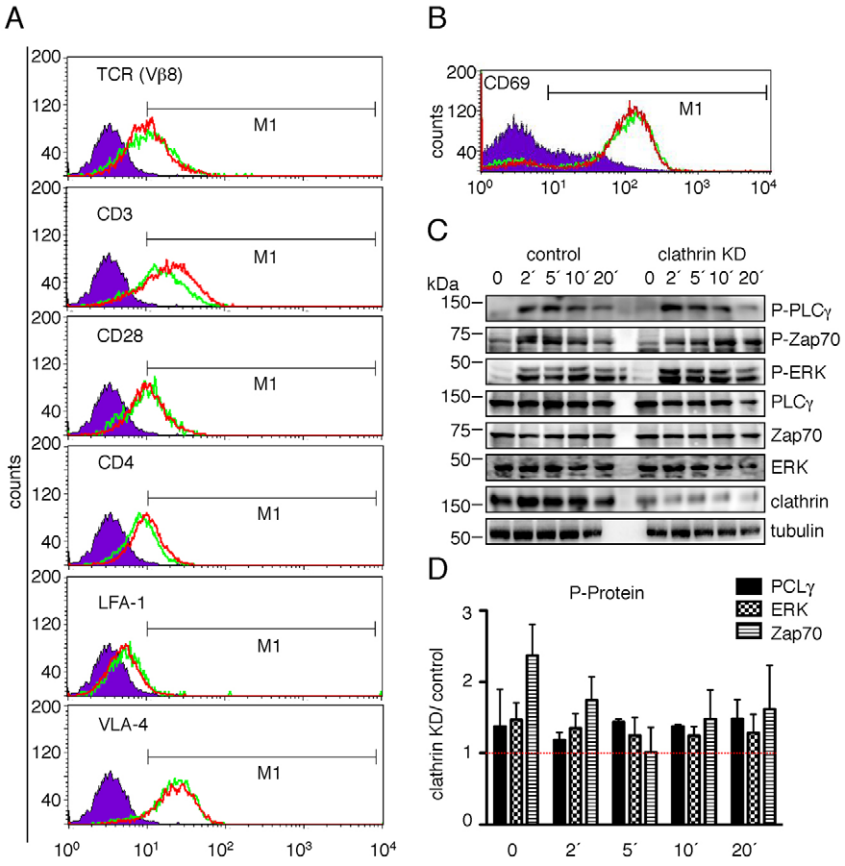

Fig. 4. Clathrin knockdown does not impede IS-induced signaling or surface expression of proteins involved in IS formation. (**A**,**B**) Surface expression of the indicated proteins was immunodetected in non-permeabilized Jurkat T cells using the corresponding primary antibodies and an Alexa-Fluor-488-labeled secondary antibody. Green lines represent staining in control T cells, and red lines represent staining in clathrin KD T cells. The blue histogram shows the fluorescent background observed with a non-specific primary antibody. Representative flow cytometry assays are shown of 13 (A) and three (B) independent experiments. Note that the faint increment in CD3 surface expression observed in clathrin KD T cells was significant; $P<0.05$ as revealed by Wilcoxon test (SPSS v. 15.0). M1 is considered the signal clearly over background. (**C**) Immunoblot detection of the phosphorylation of the indicated proteins in control and clathrin KD T cells stimulated for the indicated times with anti-CD3 and anti-CD28 antibodies. Total protein expression of the indicated proteins and tubulin was detected to control for even loading. (**D**) Clathrin KD to control ratio of phosphorylated proteins from T cells activated with CD3 and CD28 at the indicated times. Protein band density was quantified using ImageJ and signal from phosphorylated proteins were normalized to total protein. Bars corresponding to analyzed proteins (PLCγ, ERK and Zap70) show values greater than 1 in almost all time points, indicating increased signaling in clathrin KD T cells. A minimum of three independent experiments were analyzed for each protein. Data were analyzed with Prism software; error bars represent s.e.m.

polymerization (Badour et al., 2003), also accumulated at the IS in non-silenced SEE-challenged T cells, and this accumulation was impaired in clathrin KD T cells (Fig. 5E). Remarkably, clathrin depletion also abolished IS-directed relocalization of Huntingtin-interacting protein-1-related protein (Hip1R), which regulates interactions between clathrin-coated membranes and the actin cytoskeleton (Engqvist-Goldstein et al., 2004; Wilbur et al., 2008) (Fig. 5F). To verify that accumulation of clathrin, actin, dynamin-2, Arp2/3 complex, CD2AP and Hip1R at the IS was specific and to validate the Synapsis Measures software, we analyzed the cytoplasmic accumulation of GFP and CD45, a membrane tyrosine phosphatase, which after initial cell–cell contact does not accumulate at the IS (Blanchard et al., 2002; Freiberg et al., 2002; Varma et al., 2006), in T-cell–APC conjugates in the presence and absence of antigen. Endogenous CD45 and GFP did not accumulate at the IS after antigen stimulation in control or clathrin KD T cells (supplementary material Fig. S3). As expected, actin accumulated at the IS in control but not in clathrin KD T cells, and there was no significant difference in TCR accumulation at the IS between control and clathrin KD Jurkat T cells. These data confirm the active and specific accumulation at the IS of clathrin, actin and actin-polymerization promoters. Nevertheless, a remaining question is the source of clathrin promoting such actin polymerization at the IS.

Actin rearrangements at the immunological synapse are driven by endosomal clathrin

Our fluorescence microscopy data suggest that clathrin at the IS associates with internal membranes and not with the plasma membrane (Fig. 1A and supplementary material Fig. S2). Clathrin has been detected in association with cellular organelles such as the Golgi complex and MVBs (Jaiswal et al., 2009; Murk et al., 2003; Raiborg et al., 2002), as well as at the plasma membrane. To identify the source of the clathrin pool that drives actin polymerization at the IS, we monitored the association of actin with markers of the Golgi and MVB during IS formation. Giantin, a Golgi marker (Linstedt and Hauri, 1993) did not colocalize with actin (Fig. 6A). The characteristic multivesicular appearance of MVBs on electron micrographs is driven by the ESCRT (endosomal sorting complex required for transport) machinery, which inserts vesicles into late endosomes (Linstedt and Hauri, 1993). In contrast to giantin, two ESCRT components, Hrs and Vps4 (Slagsvold et al., 2006; Williams and Urbe, 2007), localized with actin at the IS in SEE-stimulated T cells (Fig. 6A, middle and bottom panels), whereas in unstimulated T cells, these MVB markers were localized in vesicles all around the cell, and did not accumulate at cell–cell contacts (supplementary material Fig. S4A). These data confirm previous studies indicating that some interactions might occur between the IS and the MVBs. For example, lyso-bis-phosphatidic acid, a marker for MVBs, (Kobayashi et al., 1998), has been recently detected in the IS (Varma et al., 2006).

We next studied the recruitment of clathrin to T cells depleted of AP-1, AP-2 or Hrs (Fig. 6B), which are adaptor molecules for the association of clathrin with the Golgi, plasma membrane and MVB, respectively (Owen et al., 2004). None of the siRNAs used affected surface expression of TCR, CD3, CD28, CD4, LFA-1 or VLA-4 (not shown). Knockdown of Hrs, and to a limited extent AP-1, impaired clathrin accumulation at the IS, whereas knockdown of the plasma membrane adaptor AP-2 had no effect (Fig. 6C). A similar dependence on Hrs was seen for actin accumulation at the

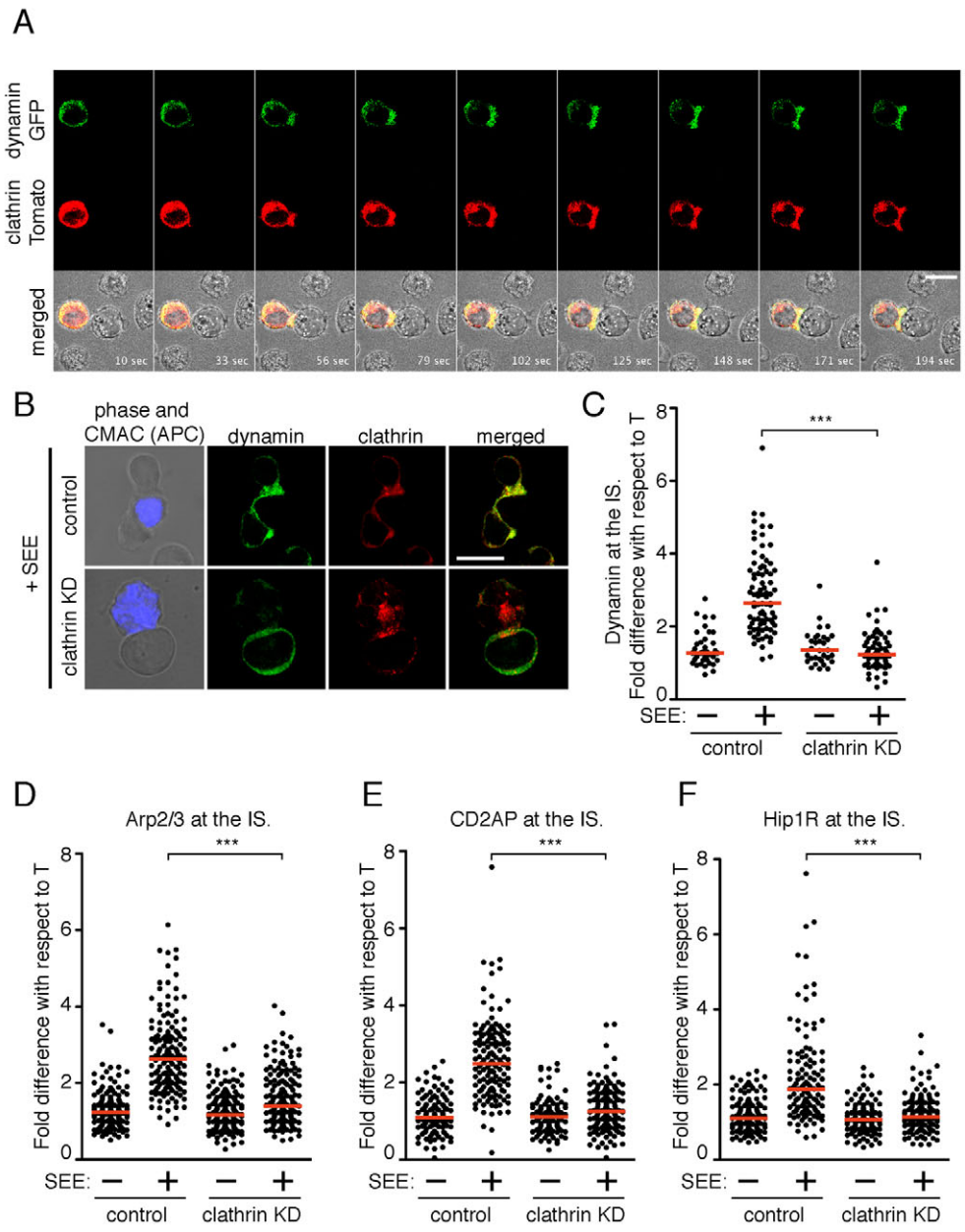

Fig. 5. Clathrin is required for the recruitment of dynamin-2 to the IS. (**A**) Confocal time series of Jurkat T cell transiently expressing td-Tomato–LCa (red) and dynamin-2–GFP (green) contacting an APC (not colored). The figure shows one of every 25 acquisition frames from supplementary material Movie 3. (**B**) Localization of endogenous clathrin (red) and dynamin-2 (green) in control or clathrin KD T cells forming conjugates with SEE-loaded APCs. Clathrin antibody used was rabbit polyclonal raised against clathrin heavy chain. APCs are stained blue; T cells are not stained. Clathrin depletion clearly impeded dynamin-2 accumulation at the IS. Scale bars: 10 µm. (**C**–**F**) Quantitative analysis using Synapse Measures of the accumulation of dynamin-2, Arp 2/3, CD2AP and Hip1R at the cell–cell contact. Control or clathrin-silenced (clathrin KD) T cells were conjugated with superantigen (SEE)-loaded (+) or unloaded (–) APCs. Each dot corresponds to an individual T-cell–APC contact. More than 250 cellular contacts were analyzed in each case in three independent experiments. ***P<0.005 (Mann–Whitney test). Red lines indicate the median values.

IS; depletion of Hrs inhibited actin accumulation, whereas no major changes could be observed in cells depleted of AP-1 or AP-2 (Fig. 6D). The role of Hrs in actin accumulation at the IS was verified with an independent set of siRNAs targeting Hrs (supplementary material Fig. S4B). The mild alteration to actin polymerization in AP-1-depleted cells suggests a minor role of the Golgi in actin accumulation at the IS; however, these experiments indicate that clathrin associated with MVBs is the main source for the recruitment of proteins that promote actin polymerization during IS formation. Consistent with this view, typical MVB structures accumulated in T cells in close contact with SEE-loaded APCs (Fig. 6E).

To confirm the role of clathrin and MVBs in actin accumulation at the IS in primary T cells, clathrin heavy chain and Hrs were knocked down by siRNA (Fig. 7A). In the presence of SEE-loaded Raji APCs, actin clearly accumulated at the IS, whereas depletion of clathrin or Hrs in T cells impaired such actin accumulation at the IS (Fig. 7B,C). Depletion of clathrin or Hrs also impeded actin accumulation at the IS in conjugates formed by primary T lymphoblasts and DCs (Fig. 7D and supplementary material Fig. S5). Note that clathrin- and Hrs- depleted primary T cells present the same levels of total actin as seen in cells with normal amounts of clathrin and Hrs (Fig. 7A). TCR accumulation (visualized by immunofluorescence with anti-Vβ8 chain antibodies) at the T-cell–APC contact site appeared unaffected, suggesting that T cell activation is not impaired by partial depletion of clathrin or Hrs in primary T cells (Fig. 7B).

Discussion

The present study provides compelling evidence that endosomal clathrin is essential for massive actin polymerization at the IS formed between T cells and APCs. Clathrin is the major protein involved in clathrin-mediated endocytosis, where it forms a coat around the pinching membrane and enables multiple protein

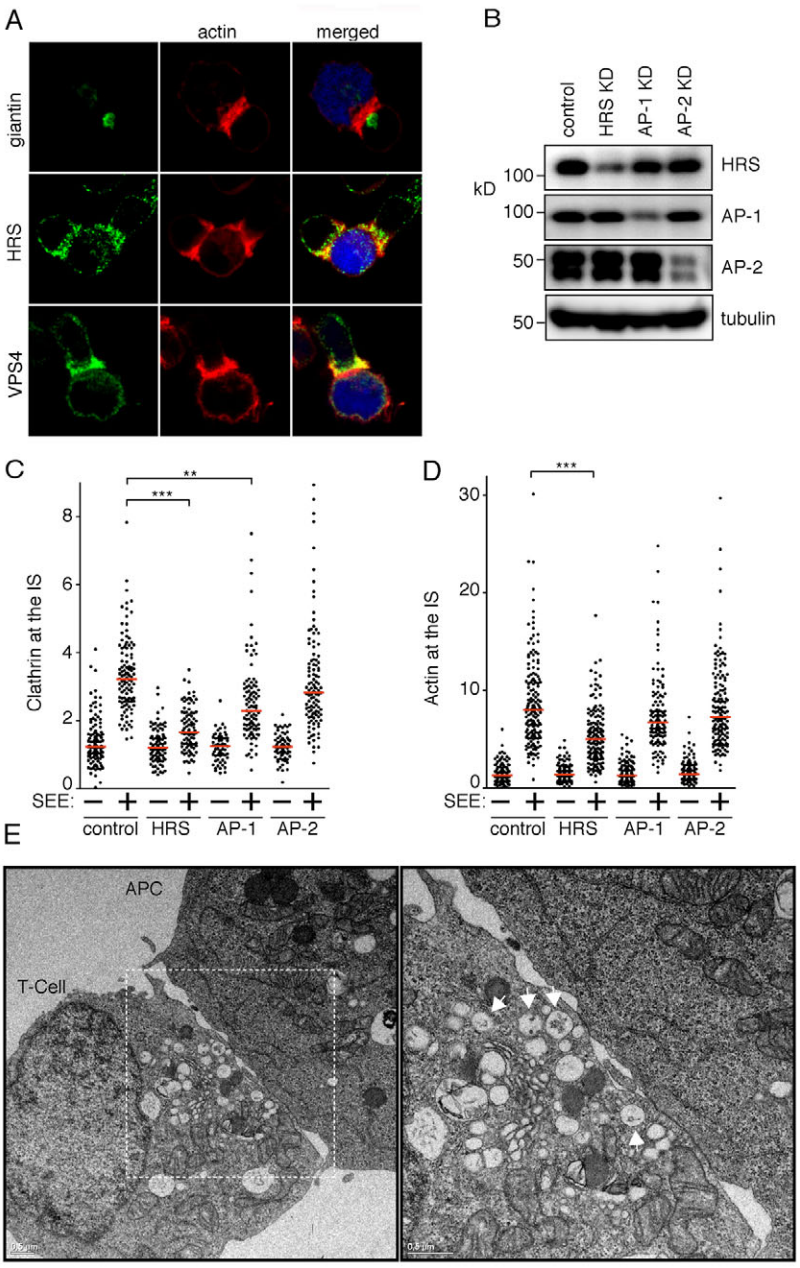

Fig. 6. Multivesicular bodies accumulate at the IS. (**A**) Confocal immunofluorescence images showing the cellular localization of giantin (Golgi marker) upper panels, HRS and VPS4 (MVB markers) middle lower panels, respectively (all in green) and actin (red) at the IS. APCs are identified in the merged image by the blue CMAC fluorescence. (**B**) Immunoblot showing suppression of Jurkat T cell protein expression of Hrs, AP-1 and AP-2 by siRNA knockdown (KD). (**C**,**D**) Control, Hrs KD, AP-1 KD and AP-2 KD T cells were conjugated with SEE-loaded (+) or unloaded (–) APCs, and Synapse Measures was used to analyze accumulation of immunostained clathrin (C) and actin (D) at the cell–cell contact area. Each dot corresponds to an individual T-cell–APC contact. More than 300 (C) or 400 (D) cellular contacts were analyzed in three independent experiments. ***P<0.005; **P<0.05 (Mann–Whitney test). Red lines indicate the median values. (**E**) Electron micrograph of the IS. The image on the right shows a high-magnification view of boxed region in the left image. Arrows indicate multivesicular bodies close to the cell–cell contact.

interactions that are necessary for endocytosis to proceed (Ungewickell and Hinrichsen, 2007). It is well established that clathrin-mediated endocytosis in yeast requires actin rearrangement (Engqvist-Goldstein and Drubin, 2003). However, the situation in mammalian cells is less clear: whereas many authors show data involving actin in clathrin-dependent endocytosis (Chen and Brodsky, 2005; Engqvist-Goldstein et al., 2004; Ferguson et al., 2009; Toshima et al., 2005; Yarar et al., 2005), others show that actin depletion has no effect on the internalization dynamics of clathrin-coated vesicles (Boucrot et al., 2006). Studies with bacterial and fungal pathogens show that clathrin and actin both participate in pathogen internalization (Moreno-Ruiz et al., 2009; Veiga and Cossart, 2005; Veiga et al., 2007), and it has been proposed that mammalian cells support internalization of large membrane plaques in a process involving clathrin and actin that is very similar to ‘classical’ clathrin-mediated endocytosis (Saffarian et al., 2009).

There are two known connections between actin and clathrin assemblies. One involves dynamin 2 and cortactin, which activates the actin nucleation factor Arp2/3 (McNiven et al., 2000; Uruno et al., 2001; Weaver et al., 2001). The other is Hip1R, which contains binding sites for F-actin, cortactin and clathrin light chains (Engqvist-Goldstein et al., 2004; Wilbur et al., 2008). A recent study shows that Hip1R is necessary for actin recruitment to clathrin-coated pits during endocytosis in *Dictyostelium discoideum* (Brady et al., 2010). However, *D. discoideum* Hip1R does not have a cortactin-binding motif and therefore these results might not be applicable to mammalian cells. Our results not only confirm that clathrin participates in biological events requiring massive actin polymerization, but also demonstrate that clathrin serves as a molecular platform to recruit the necessary proteins able to polymerize actin (dynamin-2, CD2AP and Arp2/3) at the IS. We also show that clathrin is necessary to recruit Hip1R to the IS, but

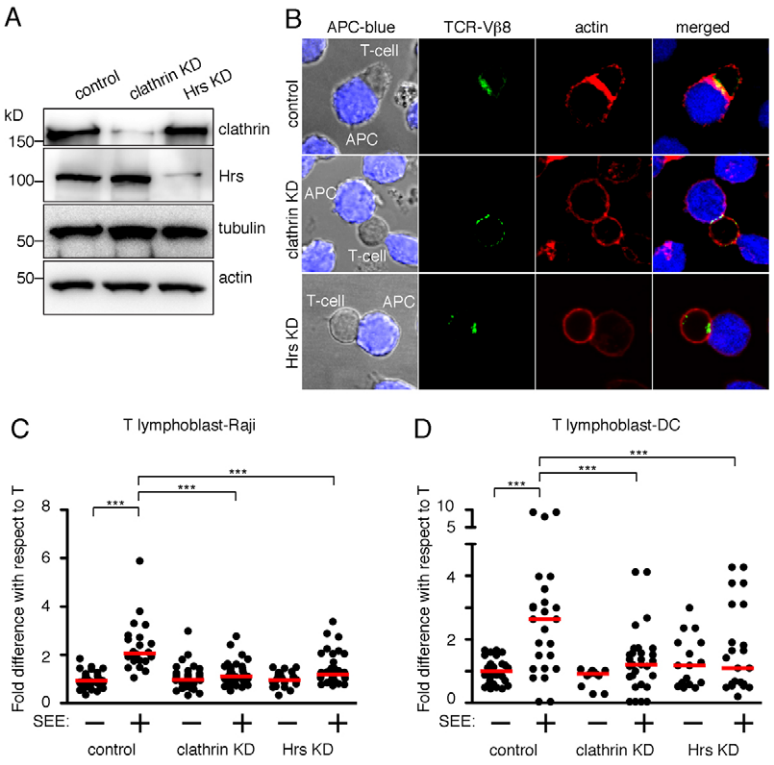

Fig. 7. Clathrin and Hrs are necessary for actin accumulation at the IS in primary T lymphoblasts. (**A**) Immunoblot showing suppression of clathrin or Hrs protein expression in knockdown (KD) T lymphoblasts. Total actin and tubulin are shown as loading controls. (**B**) Confocal immunofluorescence images of T lymphoblasts conjugated with Raji APCs. Raji cells are marked with CMAC and are shown in blue, the TCR (Vβ8 chain) is shown green, and actin in red. Merged images show actin, TCR and APCs. The upper panels show IS formed by control T lymphoblasts, the middle and lower panels show ISs formed by clathrin KD or Hrs KD T lymphoblasts, respectively. Note that depletion of clathrin or Hrs did not affect the TCR accumulation at the IS. Scale bars: 10 µm. (**C**,**D**) Quantitative analysis of actin accumulation at the cell–cell contact with Synapse Measures. Control, clathrin KD or Hrs KD T lymphoblasts were conjugated with superantigen (SEE)-loaded (+) or unloaded (–) Raji (C) or primary DCs (D). Each dot represents the relative actin immunofluorescence intensity in an individual T-cell–APC contact. T lymphoblasts and DCs were collected from three healthy donors and results shown correspond to three independent experiments. ***P<0.005 (Mann–Whitney test). Red lines indicate the median values.

understanding the role played by Hip1R at the IS requires further investigation. Notably, clathrin depletion did not reduce the surface exposure of the main membrane receptors involved in IS formation, the number of T-APC conjugates or the TCR signalling. Note that CD3 surface expression appeared to be slightly increased in clathrin KD T cells, suggesting that a fraction of CD3 molecules is internalized by clathrin-mediated endocytosis in non-stimulated cells. In this regard, it has been shown that after CD3 stimulation, endocytosis of non-engaged (bystander) TCRs is clathrin dependent, in contrast to engaged TCRs where endocytosis was clathrin independent (Monjas et al., 2004). However, the complete view of TCR and CD3 recycling and endocytosis in resting and stimulated cells is far from understood and deserves further investigation.

IL-2 secretion appeared to be deregulated (increased) in clathrin KD cells, in a similar way to what has been shown in cells treated with low doses of cytochalasin D (Nolz et al., 2007), but the mechanisms linking the actin cytoskeleton, TCR-dependent signalling and cytokine secretion remain unclear. These data, together with the quantification of polymerized actin at the IS, show that actin polymerization occurs at low levels in clathrin and Hrs KD cells, in contrast to the extraordinary levels observed in control T cells expressing normal amounts of clathrin at MVBs. Partial inhibition of actin polymerization (using low doses of cytochalasin D) have long been known to enhance integrin function (Kucik et al., 1996), which, together with the slight increase of CD3 expression observed on the surface of clathrin KD cells, could partially explain the increase of IL-2 secretion. This increased IL-2 secretion, as well as the increased TCR-dependent signalling that occurs in clathrin KD T cells, could also be explained by recent data suggesting that the actin cytoskeleton somehow destabilizes TCR–MHC interactions, as shown by treatment with cytochalasin D and latrunculin A, which greatly prolonged TCR–MHC interactions at the IS (Huppa et al., 2010).

Our data with T cell lines and with primary T cells show that the clathrin adaptor for MVB (Hrs) has a determinant role in actin polymerization at the IS. Notably, actin accumulation at the IS occurred independently of the main clathrin adaptors in the plasma membrane and Golgi complex. The dependence of clathrin and actin localization at the IS on Hrs indicates that the main platform for the recruitment of actin polymerization promoters during IS formation is clathrin associated with MVBs, which is consistent with the polar redistribution of MVBs observed by immunofluorescence and electron microscopy. These data are in agreement with recent reports suggesting MVB recruitment to the IS. It has been shown that TSG101, an ubiquitin-binding protein that is involved in cargo sorting into MVBs, regulates IS structure (Vardhana et al., 2010). These authors also showed that lyso-bis-phosphatidic acid, typically found in MVBs (Kobayashi et al., 1998), can be detected at the cSMAC (Varma et al., 2006), suggesting that some interactions might occur between MVBs and the IS. Our data confirm the proposed association of MVB with the IS and furthermore, show a role for clathrin-rich MVBs as a platform to orchestrate massive actin polymerization. Interestingly, MVB polarization to the plasma membrane also occurs during viral budding, another process in which clathrin has a major role (Morita and Sundquist, 2004). The recruitment dynamics of clathrin, actin and dynamin occur in parallel, suggesting that the machinery needed to initiate the actin polymerization process is preformed at the surface of the MVB.

The findings presented here suggest a model for actin polymerization in which antigen stimulation induces rapid movements of clathrin-containing MVBs towards the cell–cell contact site to promote localized actin polymerization. Whether this MVB–clathrin platform has a similar role in other cellular events (e.g. migration and adhesion) that require massive polarized actin polymerization remains to be determined.

Materials and Methods

Cells

The acute human leukaemia Jurkat J77cl20 Vβ8 T cell line and the Burkitt lymphoma Raji B cell line were cultured in RPMI 1640 (Gibco) supplemented with 10% fetal bovine serum (Invitrogen) and 1% penicillin-streptomycin. Human peripheral blood mononuclear cells (PBMCs) were isolated from buffy coats obtained from healthy donors by separation on a Lymphoprep gradient (Nycomed, Oslo, Norway) according to standard procedures. Monocytes were purified from PBMC by a 30 minute adherence step at 37°C in RPMI supplemented with 10% fetal calf serum. Nonadherent cells were washed off and the adhered monocytes were immediately subjected to the DC differentiation protocol, as described (Sallusto et al., 1995). Briefly, monocytes were cultured in RPMI, 10% FCS containing IL-4 (10 ng/ml, R&D Systems, Minneapolis, MN) and 1000 U/ml GM-CSF (Peprotech, London, UK). Cells were cultured for 6 days, with cytokine re-addition every 48 hours, to obtain a population of immature DCs. Phenotypic characteristics of these cells were assessed by flow cytometry on day 6 (HLA-DR$^+$, CD1a$^+$, CD209$^+$, CD14$^-$).

Human CD4$^+$ T cells were purified from PBMCs, using MACS (magnetic-activated cell sorting) and were then stimulated with irradiated autologous PBMC preincubated with 0.1 μg/ml SEE for 48 hours, cell cultures were stimulated every 2–3 days with 20 U/ml human recombinant IL-2 and 0.5 μg/ml PHA. After 1 week of treatment, around 30% of the cells were positive for TCR-Vβ8, but this percentage was variable and dependent on the donor. Studies were performed according to the principles of the Declaration of Helsinki and were approved by the local Ethics Committee for Basic Research; informed consent was obtained from all human volunteers.

Plasmids

The plasmid encoding dynamin-2–GFP (the dynamin isoform aa) was a gift from Mark A. McNiven (Mayo Clinic, Rochester, MN) (Cao et al., 1998). Plasmid encoding td-Tomato–LCa (Massol et al., 2006) was a gift from Tomás Kirchausen (Harvard Medical School, Children's Hospital and Immune Disease Institute, Boston, MA). The plasmid encoding GFP–actin (Boyer et al., 2006) was a gift from Emmanuel Lemichez (Université de Nice, Nice, France).

Antibodies and reagents

Antibodies used were as follows: anti-β-actin mouse monoclonal antibody (mAb) (AC-15; Sigma); anti-AP-1 mAb (γ-adaptin; Sigma); anti-AP-2 mAb (AP-50; Becton Dickinson (BD); anti-CD2-AP rabbit polyclonal (rAb) (Abcam); anti-CD3 mAb (BD), anti-CD3 mAb [T3B; produced in the laboratory (PiL)]; anti-CD4 mAb (BD), anti-CD28 mAb (BD); anti-CD69 mAb (TP1-55; PiL); anti-clathrin heavy chain mAb (X22; from Abcam and Pierce, normally used in western blots); anti-clathrin heavy chain rAb (Abcam), normally used in immunofluorescence assays. X22 was also used for immunofluorescence with the same results (not shown); anti-dynamin-2 rAb (Abcam), anti-ERK1/2 mAb (Millipore); anti-phosphorylated ERK1/2 mAb (Cell Signaling); anti-giantin rAb (Abcam); goat anti-guinea pig (Abcam); guinea pig anti-Hip1-R (gift from David G. Drubin, University of California at Berkeley, CA); anti-HRS rAb (HGS Abcam), anti-HRS mAb (HGS; Abnova); anti-LFA-1 mAb (BD); anti-PLC-γ1 rAb (Cell Signaling); anti-P-PLC-γ1 mAb (Y783; Cell Signaling); anti-TCR mAb (Vβ8 chain; BD); anti-tubulin mAb (Sigma); anti-Vps4 mAb (gift from Alberto Fraile, Centro Nacional de Biotecnología (CSIC), Madrid, Spain); anti-α4-integrin mAb (PiL), anti-β1-integrin mAb (PiL); anti-Zap70 mAb (Abcam); and anti-P-Zap70 mAb (Y493; Abcam). Phalloidin and goat anti-rabbit and goat anti-mouse antibodies conjugated to Alexa Fluor 488, 546 or 647 were purchased from Molecular Probes. FITC-conjugated F(ab′)2 fragment of goat anti-mouse Ig was from DakoCytomation. Cell trackers CMAC and CMTMR were purchased from Invitrogen, SEE from Toxin Technologies, cytochalasin D and glutaraldehyde from Sigma, durcupan resin from Fluka, and paraformaldehyde and osmium tetroxide from Electron Microscopy Sciences.

siRNA

Clathrin expression was suppressed by transfection of Jurkat cells with either a double-stranded RNA directed against clathrin heavy chain [sense (s) 5′-GGC CCA GGU GGU AAU CAU Utt-3′; antisense (as) 5′-AAU GAU UAC CAC CUG GGC Ctg-3′] or with an On-Target SMART pool against clathrin heavy chain (Dharmacon). AP-1 was knocked down with a single double-stranded RNA sequence (s 5′-GUU AAG CGG UCC AAC AUU Utt-3′, as 5′-AAA UGU UGG ACC GCU UAA Ctt-3′). Two sequences were used to knock down AP-2 (s 5′-GUU AAG CGG UCC AAC AUU Utt-3′, as 5′-AAA UGU UGG ACC GCU UAA Ctt-3′ and s 5′-CGC AGA GGG UAU CAA GUA Utt-3′, as 5′-AUA CUU GAU ACC CUC UGC Gtt-3′). Hrs was knocked down either with a pair of RNA sequences (s 5′-CGA CAA GAA CCC ACA CGU Ctt-3′, as 5′-GAC GUG UGG GUU CUU GUC Gtt-3′ together with s 5′-AAG CGG AGG GAA AGG CCA CUUtt-3′, as 5′-AAG UGG CCU UUC CCU CCG CUUtt-3′) or with an On-Target SMART pool (HGS) from (Dharmacon). Control sequences were On-Target plus non targeting siRNA 1 and 2 (Dharmacon) and the sequence s 5′-UUC UCC GAA CGU GUC ACG Utt-3′, as 5′-ACG UGA CAC GUU CGG AGA Att-3′. All double-stranded RNAs were purchased from Ambion or Dharmacon. Typically 400 μl of 1 μM siRNA (0.4 nmoles) were electroporated into 20×10^6 cells. Experiments were performed 48 hours after RNA transfection.

Human T lymphoblasts were silenced either by electroporation or nucleofection. T lymphoblasts were electroporated twice with a delay of 24 hours. Cells were used for experiments on day four, which corresponded to maximal silencing.

Flow cytometry

Raji B cells, labeled with 5 μM CMTMR, were loaded with 1 mg/ml SEE. Unloaded or SEE-loaded Raji cells were conjugated with Jurkat T cells at a 1:1 ratio. Primary antibodies were added in the cold (4°C) for 30 minutes. FITC-labeled goat anti-mouse Ig secondary antibody was added for 15 minutes at 4°C. Conjugates were examined with a FACSCalibur flow cytometer (BD-Biosciences) and the data were analyzed with CELLQuest software (BD Biosciences).

Immunolabeling

Conjugates were fixed in 3% paraformaldehyde in PBS, and cells were permeabilized with 0.5% Triton X-100 in PBS (5 minutes) and then incubated with the indicated antibodies. Actin was stained with an Alexa-Fluor-conjugated (488, 568 or 647 depending on the experiment) phalloidin.

Confocal microscopy

Confocal images were acquired with a Leica TCS-SP5 confocal microscope (63×) under the control of a Leica LAS AF. The images were processed with ImageJ (1.38; http://rsbweb.nih.gov/ij/index.html).

Synapse measures

Quantification of the amount of clathrin (or any protein) at the T cell side of the IS (S) with respect to the amount in the rest of the T cell (T) presents a difficult problem. First, simply computing the ratio between the average pixel values at the synapse and at the T cell border does not account for the contribution to both averages of the background (Bg) fluorescence; and second, part of the fluorescence at the synapse is caused by the B cell (B) and the contribution of the constitutive fluorescence of the T cell border. To separate all these contributions, we measured the average intensity value of the image in small circles, as shown in Fig. 1B. For measurements covering more than one region (B, T, S), the circles were placed in such a way that each region (e.g. B cell and background in the case of the B measurements) occupied approximately one half of the circle area. Taking many measurements of each kind tends to compensate for the differences in area due to the manual placement of the circles. For each kind of measurement (Bg, B, T and S), we computed the pixel value average within the multiple circles associated with that region within the same image. As a result of the location of the circle, half of the fluorescence values from the B measurements are caused by the background fluorescence whereas the other half are caused by the constitutive fluorescence of the B cells plus the background fluorescence. The same idea applies to the T measurements. The S measurements have contributions from the background, half of the constitutive fluorescence of the B-cells, and half of the fluorescence of the extra amount of clathrin present at the synapse coming from the T cell. We can express these ideas algebraically as:

$$\begin{pmatrix} Bg \\ B \\ T \\ S \end{pmatrix} = \begin{pmatrix} 1 & 0 & 0 & 0 \\ 1 & \frac{1}{2} & 0 & 0 \\ 1 & 0 & \frac{1}{2} & 0 \\ 1 & \frac{1}{2} & 0 & \frac{1}{2} \end{pmatrix} \begin{pmatrix} \widehat{Bg} \\ \hat{B} \\ \hat{T} \\ \hat{T}_s \end{pmatrix}, \tag{1}$$

where Bg, B, T and S are the average values of our measurements, $\widehat{Bg}$ is an estimate of the expected background fluorescence, $\hat{B}$ is an estimate of the constitutive fluorescence of the B-cells, $\hat{T}$ is an estimate of the constitutive fluorescence of the T cells outside the synapse, and $\hat{T}_s$ is an estimate of the constitutive fluorescence of the T cells at the synapse. From the measurement model, the estimates can be easily derived as:

$$\begin{pmatrix} \widehat{Bg} \\ \hat{B} \\ \hat{T} \\ \hat{T}_s \end{pmatrix} = \begin{pmatrix} 1 & 0 & 0 & 0 \\ -2 & 2 & 0 & 0 \\ -2 & 0 & 2 & 0 \\ 0 & -2 & 0 & 2 \end{pmatrix} \begin{pmatrix} Bg \\ B \\ T \\ S \end{pmatrix}. \tag{2}$$

From this we can estimate the ratio between the fluorescence at the T cell synapse and in T cell regions outside the synapse as $Z=T_s/T$. This ratio is computed for each IS image.

Statistical analysis

Differences between groups were analyzed by the Mann–Whitney U-test (unless otherwise noted). Differences were considered significant at $P\leq0.05$. Unless otherwise stated, all experiments were performed at least three times, and data are presented as median values.

Cytochalasin treatment

J77 T cells were incubated with 10 μM cytochalasin in DMSO for 30 minutes at 37°C. J77 cells were then conjugated for 15 minutes with SEE-primed or unprimed Raji B cells at 37°C, and conjugates were fixed in 3% paraformaldehyde in PBS.

IL-2 secretion analysis

Conjugates were formed and cultured in flat-bottom, 96-well plates. Culture supernatant was harvested after culture for 16 hours and analyzed for IL-2 concentration by ELISA (Diaclone, Gen-Probe-TDI, Stamford, CT).

Live-cell Imaging

Jurkat T cells expressing td-Tomato–LCa, GFP–actin or dynamin-2–GFP were resuspended in HBSS containing 2% FBS and seeded in a glass-bottomed dish. SEE-loaded CMAC-labelled Raji APCs were added, and conjugate formation was monitored for 15 minutes. Images were acquired with a Leica TCS-SP5 confocal microscope equipped with a resonant scanner under the control of Leica LAS AF software. Three confocal planes were acquired approximately every second. Resulting images were processed with ImageJ 1.38 (http://rsbweb.nih.gov/ij/index.html). The movies presented show the maximal projection of the three confocal planes.

Electron microscopy

T-cell–APC conjugates were fixed in 2.5% glutaraldehyde in PBS for 30 minutes, and the fixation buffer was then substituted with 1% osmium tetroxide for 45 minutes. Samples were dehydrated through a series of ethanol solutions (5%, 25%, 50%, 75%, 95% and 100%). After the last dehydration step, samples were embedded in DURCUPAN resin and stored overnight at room temperature. The resin column was then polymerized by baking at 60°C for 48 hours, after which sections were cut. Sections were examined with a JEOL JEM1010 electron microscope (100 kV) equipped with a BioScan digital camera (Gatan). Images were monitored with DigitalMicrograph 3.1 (Gatan).

We are grateful to Mark A. McNiven, Tomás Kirchhausen, Alberto Fraile and Emmanuel Lemichez for providing reagents. We thank Simon Bartlett for help with English editing. The assistance of Monica Torres is greatly appreciated. This work has been partly supported by the Grants: RYC-2007-01822, BFU 2008-04342/BMC, SAF-2008-02635, INSINET 01592006 CAM, Red RECAVA RD06/0014-0030, FONCICYT-C002-2008-1 ALA/127249 and FIPSE 36658/07. The authors do not have any conflict of interest that might influence the results or interpretation of this manuscript.

Supplementary material available online at
http://jcs.biologists.org/cgi/content/full/124/5/820/DC1

References

Badour, K., Zhang, J., Shi, F., McGavin, M. K., Rampersad, V., Hardy, L. A., Field, D. and Siminovitch, K. A. (2003). The Wiskott-Aldrich syndrome protein acts downstream of CD2 and the CD2AP and PSTPIP1 adaptors to promote formation of the immunological synapse. *Immunity* **18**, 141-154.

Billadeau, D. D., Nolz, J. C. and Gomez, T. S. (2007). Regulation of T-cell activation by the cytoskeleton. *Nat. Rev. Immunol.* **7**, 131-143.

Blanchard, N., Di Bartolo, V. and Hivroz, C. (2002). In the immune synapse, ZAP-70 controls T cell polarization and recruitment of signaling proteins but not formation of the synaptic pattern. *Immunity* **17**, 389-399.

Boucrot, E., Saffarian, S., Massol, R., Kirchhausen, T. and Ehrlich, M. (2006). Role of lipids and actin in the formation of clathrin-coated pits. *Exp. Cell Res.* **312**, 4036-4048.

Boyer, L., Doye, A., Rolando, M., Flatau, G., Munro, P., Gounon, P., Clément, R., Pulcini, C., Popoff, M. R., Mettouchi, A. et al. (2006). Induction of transient macroapertures in endothelial cells through RhoA inhibition by Staphylococcus aureus factors. *J. Cell Biol.* **173**, 809-819.

Brady, R. J., Damer, C. K., Heuser, J. E. and O'Halloran, T. J. (2010). Regulation of Hip1r by epsin controls the temporal and spatial coupling of actin filaments to clathrin-coated pits. *J. Cell Sci.* **123**, 3652-3661.

Cao, H., Garcia, F. and McNiven, M. A. (1998). Differential distribution of dynamin isoforms in mammalian cells. *Mol. Biol. Cell* **9**, 2595-2609.

Chen, C.-Y. and Brodsky, F. M. (2005). Huntingtin-interacting protein 1 (Hip1) and Hip1-related protein (Hip1R) bind the conserved sequence of clathrin light chains and thereby influence clathrin assembly in vitro and actin distribution in vivo. *J. Biol. Chem.* **280**, 6109-6117.

Conner, S. D. and Schmid, S. L. (2003). Regulated portals of entry into the cell. *Nature* **422**, 37-44.

Dustin, M. L. (2009). The cellular context of T cell signaling. *Immunity* **30**, 482-492.

Engqvist-Goldstein, A. E. and Drubin, D. (2003). Actin assembly and endocytosis: from yeast to mammals. *Annu. Rev. Cell Dev. Biol.* **19**, 287-332.

Engqvist-Goldstein, A. E., Zhang, C. X., Carreno, S., Barroso, C., Heuser, J. and Drubin, D. (2004). RNAi-mediated Hip1R silencing results in stable association between the endocytic machinery and the actin assembly machinery. *Mol. Biol. Cell* **15**, 1666-1679.

Ferguson, S. M., Ferguson, S., Raimondi, A., Paradise, S., Shen, H., Mesaki, K., Ferguson, A., Destaing, O., Ko, G., Takasaki, J. et al. (2009). Coordinated actions of actin and BAR proteins upstream of dynamin at endocytic clathrin-coated pits. *Dev. Cell* **17**, 811-822.

Freiberg, B. A., Kupfer, H., Maslanik, W., Delli, J., Kappler, J., Zaller, D. M. and Kupfer, A. (2002). Staging and resetting T cell activation in SMACs. *Nat. Immunol* **3**, 911-917.

Friedl, P., den Boer, A. T. and Gunzer, M. (2005). Tuning immune responses: diversity and adaptation of the immunological synapse. *Nat. Rev. Immunol.* **5**, 532-545.

Gomez, T. S., Hamann, M. J., McCarney, S., Savoy, D. N., Lubking, C. M., Heldebrant, M. P., Labno, C. M., McKean, D. J., Mcniven, M., Burkhardt, J. K. et al. (2005). Dynamin 2 regulates T cell activation by controlling actin polymerization at the immunological synapse. *Nat. Immunol.* **6**, 261-270.

Hamon, M., Bierne, H. and Cossart, P. (2006). *Listeria monocytogenes*: a multifaceted model. *Nat. Rev. Microbiol.* **4**, 423-434.

Hanson, P. I., Shim, S. and Merrill, S. A. (2009). Cell biology of the ESCRT machinery. *Curr. Opin. Cell Biol.* **21**, 568-574.

Huppa, J. B., Axmann, M., Mörtelmaier, M. A., Lillemeier, B. F., Newell, E. W., Brameshuber, M., Klein, L. O., Schütz, G. J. and Davis, M. M. (2010). TCR-peptide-MHC interactions in situ show accelerated kinetics and increased affinity. *Nature* **463**, 963-967.

Jaiswal, J. K., Rivera, V. M. and Simon, S. M. (2009). Exocytosis of post-Golgi vesicles is regulated by components of the endocytic machinery. *Cell* **137**, 1308-1319.

Kobayashi, T., Stang, E., Fang, K. S., de Moerloose, P., Parton, R. G. and Gruenberg, J. (1998). A lipid associated with the antiphospholipid syndrome regulates endosome structure and function. *Nature* **392**, 193-197.

Kucik, D. F., Dustin, M. L., Miller, J. M. and Brown, E. J. (1996). Adhesion-activating phorbol ester increases the mobility of leukocyte integrin LFA-1 in cultured lymphocytes. *J. Clin. Invest.* **97**, 2139-2144.

Linstedt, A. D. and Hauri, H. P. (1993). Giantin, a novel conserved Golgi membrane protein containing a cytoplasmic domain of at least 350 kDa. *Mol. Biol. Cell* **4**, 679-693.

Massol, R. H., Boll, W., Griffin, A. M. and Kirchhausen, T. (2006). A burst of auxilin recruitment determines the onset of clathrin-coated vesicle uncoating. *Proc. Natl. Acad. Sci. USA* **103**, 10265-10270.

McNiven, M. A., Kim, L., Krueger, E. W., Orth, J. D., Cao, H. and Wong, T. W. (2000). Regulated interactions between dynamin and the actin-binding protein cortactin modulate cell shape. *J. Cell Biol.* **151**, 187-198.

Mittelbrunn, M., Molina, A., Escribese, M. M., Yanez-Mo, M., Escudero, E., Ursa, A., Tejedor, R., Mampaso, F. and Sanchez-Madrid, F. (2004). VLA-4 integrin concentrates at the peripheral supramolecular activation complex of the immune synapse and drives T helper 1 responses. *Proc. Natl. Acad. Sci. USA* **101**, 11058-11063.

Monjas, A., Alcover, A. and Alarcón, B. (2004). Engaged and bystander T cell receptors are down-modulated by different endocytotic pathways. *J. Biol. Chem.* **279**, 55376-55384.

Montoya, M. C., Sancho, D., Bonello, G., Collette, Y., Langlet, C., He, H. T., Aparicio, P., Alcover, A., Olive, D. and Sanchez-Madrid, F. (2002). Role of ICAM-3 in the initial interaction of T lymphocytes and APCs. *Nat. Immunol.* **3**, 159-168.

Moreno-Ruiz, E., Galan-Diez, M., Zhu, W., Fernandez-Ruiz, E., d'Enfert, C., Filler, S. G., Cossart, P. and Veiga, E. (2009). Candida albicans internalization by host cells is mediated by a clathrin-dependent mechanism. *Cell. Microbiol.* **11**, 1179-1189.

Morita, E. and Sundquist, W. (2004). Retrovirus budding. *Annu. Rev. Cell Dev. Biol.* **20**, 395-425.

Murk, J. L., Humbel, B. M., Ziese, U., Griffith, J. M., Posthuma, G., Slot, J. W., Koster, A. J., Verkleij, A. J., Geuze, H. J. and Kleijmeer, M. J. (2003). Endosomal compartmentalization in three dimensions: implications for membrane fusion. *Proc. Natl. Acad. Sci. USA* **100**, 13332-13337.

Nolz, J. C., Fernandez-Zapico, M. E. and Billadeau, D. D. (2007). TCR/CD28-stimulated actin dynamics are required for NFAT1-mediated transcription of c-rel leading to CD28 response element activation. *J. Immunol.* **179**, 1104-1112.

Owen, D., Collins, B. and Evans, P. (2004). Adaptors for clathrin coats: structure and function. *Annu. Rev. Cell Dev. Biol.* **20**, 153-191.

Perez-Martinez, M., Gordon-Alonso, M., Cabrero, J. R., Barrero-Villar, M., Rey, M., Mittelbrunn, M., Lamana, A., Morlino, G., Calabia, C., Yamazaki, H. et al. (2010). F-actin-binding protein drebrin regulates CXCR4 recruitment to the immune synapse. *J. Cell Sci.* **123**, 1160-1170.

Raiborg, C., Bache, K., Gillooly, D., Madshus, I., Stang, E. and Stenmark, H. (2002). Hrs sorts ubiquitinated proteins into clathrin-coated microdomains of early endosomes. *Nat. Cell Biol.* **4**, 394-398.

Raiborg, C., Wesche, J., Malerød, L. and Stenmark, H. (2006). Flat clathrin coats on endosomes mediate degradative protein sorting by scaffolding Hrs in dynamic microdomains. *J. Cell Sci.* **119**, 2414-2424.

Reichardt, P., Dornbach, B. and Gunzer, M. (2007). The molecular makeup and function of regulatory and effector synapses. *Immunol. Rev.* **218**, 165-177.

Saffarian, S., Cocucci, E. and Kirchhausen, T. (2009). Distinct dynamics of endocytic clathrin-coated pits and coated plaques. *PLoS Biol.* **7**, e1000191.

Sallusto, F., Cella, M., Danieli, C. and Lanzavecchia, A. (1995). Dendritic cells use macropinocytosis and the mannose receptor to concentrate macromolecules in the major histocompatibility complex class II compartment: downregulation by cytokines and bacterial products. *J. Exp. Med.* **182**, 389-400.

Slagsvold, T., Pattni, K., Malerod, L. and Stenmark, H. (2006). Endosomal and non-endosomal functions of ESCRT proteins. *Trends Cell Biol.* **16**, 317-326.

Toshima, J., Toshima, J. Y., Martin, A. C. and Drubin, D. G. (2005). Phosphoregulation of Arp2/3-dependent actin assembly during receptor-mediated endocytosis. *Nat. Cell Biol.* **7**, 246-254.

Ungewickell, E. J. and Hinrichsen, L. (2007). Endocytosis: clathrin-mediated membrane budding. *Curr. Opin. Cell Biol.* **19**, 417-425.

Uruno, T., Liu, J., Zhang, P., Fan, Y., Egile, C., Li, R., Mueller, S. C. and Zhan, X. (2001). Activation of Arp2/3 complex-mediated actin polymerization by cortactin. *Nat. Cell Biol.* **3**, 259-266.

Vardhana, S., Choudhuri, K., Varma, R. and Dustin, M. L. (2010). Essential role of ubiquitin and TSG101 protein in formation and function of the central supramolecular activation cluster. *Immunity* **32**, 531-540.

Varma, R., Campi, G., Yokosuka, T., Saito, T. and Dustin, M. L. (2006). T cell receptor-proximal signals are sustained in peripheral microclusters and terminated in the central supramolecular activation cluster. *Immunity* **25**, 117-127.

Veiga, E. and Cossart, P. (2005). *Listeria* hijacks the clathrin-dependent endocytic machinery to invade mammalian cells. *Nat. Cell Biol.* **7**, 894-900.

Veiga, E., Guttman, J. A., Bonazzi, M., Boucrot, E., Toledo-Arana, A., Lin, A. E., Enninga, J., Pizarro-Cerdá, J., Finlay, B. B., Kirchhausen, T. et al. (2007). Invasive and adherent bacterial pathogens co-Opt host clathrin for infection. *Cell Host Microbe* **2**, 340-351.

Vicente-Manzanares, M. and Sanchez-Madrid, F. (2004). Role of the cytoskeleton during leukocyte responses. *Nat. Rev. Immunol.* **4**, 110-122.

Weaver, A. M., Karginov, A. V., Kinley, A. W., Weed, S. A., Li, Y., Parsons, J. T. and Cooper, J. A. (2001). Cortactin promotes and stabilizes Arp2/3-induced actin filament network formation. *Curr. Biol.* **11**, 370-374.

Wilbur, J. D., Chen, C. Y., Manalo, V., Hwang, P. K., Fletterick, R. J. and Brodsky, F. M. (2008). Actin binding by Hip1 (huntingtin-interacting protein 1) and Hip1R (Hip1-related protein) is regulated by clathrin light chain. *J. Biol. Chem.* **283**, 32870-32879.

Williams, R. L. and Urbe, S. (2007). The emerging shape of the ESCRT machinery. *Nat. Rev. Mol. Cell Biol.* **8**, 355-368.

Yarar, D., Waterman-Storer, C. M. and Schmid, S. L. (2005). A dynamic actin cytoskeleton functions at multiple stages of clathrin-mediated endocytosis. *Mol. Biol. Cell* **16**, 964-975.